Biogeochemistry (2026) 169:18
https://doi.org/10.1007/s10533-026-01314-2

Can coarse woody material account for the nitrogen imbalance at Hubbard Brook Experimental Forest, New Hampshire, USA?

Andrew Ouimette · Jack Hastings · Tony D'Amato · John J. Battles · Mark Ducey · Jane R. Foster · Colin Fuss · Christine Goodale · Chris Johnson · Ashley Lang · Scott V. Ollinger

Received: 16 September 2025 / Accepted: 15 February 2026

Abstract The decay of coarse woody litter serves a potentially important role in forest nitrogen cycling. The carbon-rich, nitrogen-poor chemistry of wood allows it to immobilize, store, and in later stages of decomposition, supply nitrogen to forest ecosystems. The decay of woody litter happens over decadal time scales, making direct observations of its importance to nitrogen cycling challenging. Modeling woody litter decay can provide insights into its role in nitrogen cycling but is complex because it is influenced by microbial stoichiometric demands, wood chemistry, time spent as standing versus downed wood, input rates from mortality and disturbances, decay rates, and whether these processes are dynamic over time. One ecosystem where these uncertainties are particularly relevant is the Hubbard Brook Experimental Forest in New Hampshire, USA, where long-term monitoring of a reference watershed has revealed a persistent imbalance between nitrogen inputs and losses. Microbial immobilization of nitrogen in decaying wood has been proposed as an unaccounted-for nitrogen sink.

Responsible Editor: Edith Bai.

Supplementary Information The online version contains supplementary material available at https://doi.org/10.1007/s10533-026-01314-2.

A. Ouimette (✉)
USDA Forest Service, Northern Research Station, Durham, NH, USA
e-mail: Andrew.Ouimette@usda.gov

J. Hastings · S. V. Ollinger
Earth Systems Research Center, University of New Hampshire, Durham, NH, USA

T. D'Amato
Rubenstein School of Environment & Natural Resources, University of Vermont, Burlington, VT, USA

J. J. Battles
Department of Environmental Science Policy and Management, University of California, Berkeley, CA, USA

M. Ducey
Department of Natural Resources and the Environment, University of New Hampshire, Durham, NH, USA

J. R. Foster
USDA Forest Service, Southern Research Station, Knoxville, TN, USA

C. Fuss
Center for Earth and Environmental Science, State University of New York Plattsburgh, Plattsburgh, NY, USA

C. Goodale
Department of Ecology and Evolutionary Biology, Cornell University, Ithaca, NY, USA

C. Johnson
College of Engineering and Computer Science, Syracuse University, Syracuse, NY, USA

A. Lang
USDA Forest Service, Northern Research Station, St. Paul, MN, USA

Published online: 24 March 2026

To test whether coarse dead wood contributes to this imbalance, we modeled nitrogen and carbon dynamics during decay and the processes influencing their cycling. We found that 1) Nitrogen dynamics in dead wood likely do not account for a substantial fraction of the nitrogen imbalance observed at Hubbard Brook, and 2) Low microbial carbon-use efficiency for wood decay (<0.10) was most consistent with observed data and had a large influence on the capacity of wood to immobilize nitrogen and the fate of wood-derived carbon.

Keywords Woody decay · Model · Nitrogen · Microbial carbon-use efficiency · Coarse woody material · Hubbard Brook Experimental Forest

Introduction

Nitrogen (N) is a critical nutrient that limits forest productivity and timber production and plays a central role in governing ecosystem function. Understanding the processes that immobilize N (rendering it temporarily unavailable for plant uptake) or release N (making it accessible again) is essential for sustainable forest management, long-term soil fertility, and predicting forest responses to disturbance and succession (Harmon et al. 2004; Laiho and Prescott 2004).

At the Hubbard Brook Experimental Forest (HBEF), a mature temperate forest in the northeastern United States, a long-standing N imbalance has been observed, in which atmospheric N inputs exceed known outputs. This discrepancy is well documented in Watershed 6 (HBEF-W6), a reference watershed for biogeochemical studies. As the forest matured and net tree biomass reached near equilibrium in the early 1980s, it was expected that a declining net sink of N in biomass, combined with continued atmospheric N deposition, would result in larger dissolved N exports via streamflow. Instead, dissolved N losses have steadily declined since the 1970s, with stream nitrate now often below instrument detection limits during the growing season (Lovett et al. 2018). Gaseous losses of N appear to have decreased since the late 1990's (Groffman et al. 2018), resulting in an apparent imbalance of roughly 5.5–11.5 kg N ha^{-1} yr^{-1} after accounting for changes in biomass N storage (Yanai et al. 2013; Lovett et al. 2018).

Several hypotheses have been proposed to explain this "missing" N sink, including an unaccounted-for N sink in soils (Lovett et al. 2018) and microbial immobilization of N in coarse dead wood (Lajtha 2020). To test the latter hypothesis, we developed a process-based model to evaluate whether coarse woody material (CWM) dynamics could account for the observed N imbalance at HBEF-W6.

Coarse woody material plays a potentially underappreciated role in cycling N through temperate and boreal forests, particularly over the course of forest succession (Harmon et al. 2004; Lajtha 2020). Coarse woody material is carbon (C) rich and N poor, with the carbon to nitrogen ratio (C:N) often an order of magnitude higher than foliar, fine root, and microbial biomass. With its low N concentrations, CWM supports microbial communities that immobilize N during early stages of decay and release N in later stages of decomposition (Harmon 2021). However, a complete understanding of the impacts of CWM on N cycling is still lacking, largely due to the long timescales over which wood decay processes occur. Various studies have reported that CWM plays either an important (Wiebe et al. 2012) or minor (Laiho and Prescott 2004) role in forest N cycles, illustrating the need to advance our understanding of nutrient cycling in CWM.

In temperate and boreal forests, the decay of CWM is primarily carried out by fungi and bacteria, which typically have a low C:N (5–20), compared to CWM (250–500+) (Zechmeister-Boltenstern et al. 2015). This creates a substantial stoichiometric imbalance and high microbial demand for N. To meet this demand, N is often immobilized during the initial stages of wood decay until stoichiometric demands are met (Mooshammer et al. 2014). The C:N at which net N mineralization from decaying leaf, root, and woody litter begins has been referred to as the *critical* C:N (Berg and Staaf 1981) and depends on initial litter C:N as well as microbial carbon-use efficiency (CUE) based on synthesis studies that include, but are not dominated by CWM (Manzoni et al. 2008). Recent work has highlighted that this relationship is less well constrained for CWM than for foliar litter, with CWM often net releasing N earlier than expected (Wijas et al. 2025).

Many ecosystem models employ a critical C:N concept to simulate the decay of organic matter, allowing organic matter to immobilize N when its

C:N is above a critical C:N threshold, and to net mineralize N below the critical C:N. However, many of these models use a fixed critical C:N parameterization across organic matter types, essentially fixing the CUE of the microbial community to values typically greater than 0.20 g C of new microbial biomass per g of organic C consumed (Zhang et al. 2018). This parameterization allows net N mineralization from organic matter only when litter C:N has reached relatively low values (e.g., net mineralization only when litter C:N is less than 50 for microbial biomass with a C:N of 10 and a CUE 0.20 or greater). Contrary to these constraints, there are reports of net N mineralization occurring in high C:N (250–500) CWM with very little to no net immobilization of N (Krankina et al. 1999; Ganjegunte et al. 2004; Brais et al. 2006; Palviainen et al. 2008; Johnson et al. 2014). Further, although N is often initially immobilized in CWM, net N mineralization is typically observed at relatively high C:N, often > 150 (Grier 1978; Edmonds 1987; Sollins et al. 1987; Chen et al. 2001; Creed et al. 2004; Palviainen et al. 2008; Preston et al. 2012; Johnson et al. 2014; Smyth et al. 2016; Prescott et al. 2017; Strukelj et al. 2018).

To reconcile observations that N-rich litter can immobilize N at relatively low C:N, while N-poor coarse woody litter can net mineralize N, even at high C:N, (Manzoni 2017) proposed a conceptual model of flexible microbial CUE. In this model, microbial decomposers using N-poor litter have a lower CUE to maximize their growth rate—in other words, microbial communities on C-rich, N-poor litter reduce the fraction of C that is assimilated into biomass versus heterotrophically respired. This model is consistent with measurements of microbial CUE in both terrestrial and aquatic ecosystems (Manzoni et al. 2017) and reconciles litter decay experiments which suggest that the CUE of decomposition—the fraction of assimilated C retained in microbial biomass versus lost as respiration or other microbial processes—ranges from less than 0.1 for wood decomposers to as high as 0.5 for decomposition of N-rich, high-quality litter (Manzoni et al. 2008, 2012, 2017). Together, both observations and modeling imply that litter chemistry is a dominant control on N mineralization from decaying litter (Manzoni et al. 2017) and should be taken into account when constructing or parameterizing models of wood decay. Given the importance of initial litter chemistry in controlling decay processes, Romashkin et al. (2018, 2021) suggest it is also important to explicitly separate wood and bark components, which differ in chemistry and C:N, degree of N immobilization, and timing of net N mineralization.

In addition to the chemistry of CWM, any process that affects its supply and turnover will translate into changes in N stocks and N fluxes from CWM. For example, the supply of woody litter is controlled by the size of the live woody biomass pool and rates of tree mortality and branchfall. Decay (or mass loss) of CWM is controlled by chemistry and climate, but also by the position of dead wood, whether standing or downed. Standing dead trees often decay 2–4 times more slowly than downed dead wood due to due differences in the degree of ground contact and microclimate, with the exception of very wet ecosystems (Law et al. 2019; Harmon et al. 2020). The fraction of woody necromass found in standing versus downed pools is dependent on the fall rate of standing dead trees, which varies with mode of death, stand density, species, climate, and tree size (Garber et al. 2005; Oberle et al. 2018). Recent work also suggests that initial deadwood piece size can further influence decay rates and residence times (Wijas et al. 2025). Large inputs of CWM through disturbance events can also have lasting impacts on C and N dynamics in forests.

The extent to which wood decay progresses to completion over decades remains poorly quantified. Observations from foliar litter decay experiments suggest there is a limit to the degree of short-term decay. Specifically, Berg et al. (1996) and others have shown that some fraction of initial litter mass decomposes at very slow rates and can persist for centuries, resulting in an upper limit to how much decay can occur over annual to decadal timescales. These limit values tend to be on the order of 10–30% for foliar litter, with N-rich litter producing a greater fraction of persistent organic matter compared to N-poor litter. Although the limit value concept has important implications for C and N cycling, limit values are largely unknown for CWM, due to the long decomposition experiments required to estimate values for wood.

Finally, adding to the uncertainty and difficulty in predicting fluxes of C and N from dead wood is that many of these processes are dynamic and can

vary over time within a stand due to changes in species composition and tree size. Decay rates and snag fall rates can vary with the size of dead wood, with larger diameter woody material often (but not always) decaying and falling at slower rates than smaller diameter pieces (Harmon et al. 2020), as well as with the spatial position of dead wood within the stand. Mortality rates can also vary over the course of succession, even in the absence of large disturbances (Lines et al. 2010). The microbial community colonizing dead wood, their CUE and N requirements also likely vary during wood decay. Existing models rarely incorporate the full complexity of dead wood C and N dynamics that include all the mechanisms listed above.

Motivated by uncertainty surrounding the role of dead wood in forest N budgets, we developed a process-based model to explore how key mechanisms influence C and N fluxes from CWM at HBEF-W6 and to answer the following questions:

1) Can uncertainty in the magnitude of N cycling through CWM explain the N imbalance observed at HBEF-W6?
2) What microbial CUE best reproduces N dynamics observed during wood decay, and how does it affect N retention in CWM and the fate of wood-derived C?

We hypothesize that: 1) Nitrogen immobilization in CWM is insufficient to account for the observed N imbalance at HBEF-W6, based on prior wood-decay studies at Hubbard Brook that observed relatively rapid turnover of CWM and limited N retention during decomposition, and 2) Microbial CUE strongly controls N immobilization and C fluxes in CWM, and simulations with low CUE values (<0.10) are most consistent with observed N and C dynamics during wood decay.

Methods

Model description

The model presented here was developed to simulate cohort-level and ecosystem-scale N and C stocks and fluxes during the decay of CWM (Fig. 1). Using an annual timestep, the model first simulates live wood biomass through a user-defined wood production rate that can either remain constant or vary over time. Dead wood inputs are then generated by the turnover of live woody biomass. Wood and bark components can be tracked separately, with their initial proportions determined by a user-defined bark fraction parameter. Live wood turnover, which includes the sum of mortality and coarse branchfall,

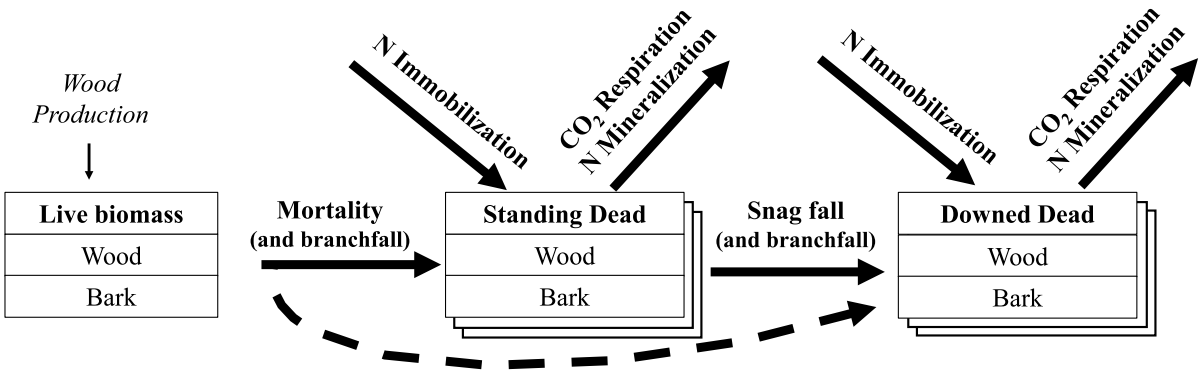

Fig. 1 Model structure developed to assess the C and N dynamics in CWM. Pools are represented as boxes, fluxes of C and N as arrows. Live woody biomass is subject to mortality that is tracked as annual cohorts and can either transition directly to standing dead wood or partially into standing and downed dead wood based on an initial fall fraction. N is immobilized in CWM until a critical C:N is reached and is then net mineralized from CWM cohorts. C is lost via microbial respiration during decay. Decay can be simulated as either a single exponential, asymptotic, or double exponential type decay by parameterizing the limit value and slow decay rate. In all stages of the model wood and bark components can either be tracked separately or as a single pool

is parameterized by a mortality rate that can either remain static or change over time.

Dead wood is partitioned into standing and downed pools based on an initial "fall fraction" parameter, requiring the model to track individual annual dead wood cohorts. Standing dead wood undergoes decay and continues to transfer to downed woody material though a user defined snag fall rate. The fall of standing dead wood over time can occur as a constant fraction of initial mass or as a declining exponential function, with a higher proportion of a standing dead cohort's mass falling in early years and decreasing exponentially over time. Standing and downed dead wood pools have distinct decay rate constants, with standing dead decaying more slowly in our simulations, although this is user configurable.

Following Berg et al. (1996), we allow for the use of a limit value to decomposition. We do this using a double exponential decay function that tracks both labile and more recalcitrant fractions of woody litter, representing relatively fast- and slow-decomposing components rather than explicit chemical constituents. The proportion of an initial dead wood cohort that begins in the recalcitrant fraction is parameterized using the limit value. With user parameterization of the limit value and the decay rate constant of this recalcitrant fraction ("slow decay rate"), wood decomposition can be simulated as single exponential decay (limit value = 0), an asymptotic decay model (limit value > 0; slow decay rate = 0), or a double exponential decay (limit value > 0; slow decay rate > 0). Labile and recalcitrant pools decay simultaneously (in parallel).

We allow CWM to immobilize N and delay net N mineralization by implicitly including microbial dynamics and stoichiometric demands. Specifically, to satisfy decomposer stoichiometric C and N demands, N is net immobilized when the C:N of decaying wood is above a critical C:N, and net mineralization occurs once dead wood cohorts are at or below the critical C:N according to Eq. (1) (Manzoni et al. 2008).

$$\text{Net } N \text{ Exchange} = -\text{Wood Decay } C \text{ Flux} \times \left(\frac{1}{\text{Wood } C{:}N} - \frac{1}{\text{Critical } C{:}N}\right)$$

$$(\text{immobilization} > 0,\ \text{mineralization} < 0) \tag{1}$$

Wood and bark components have distinct critical C:N values and thus different trajectories of N immobilization and mineralization over time. The critical C:N of wood and bark components are determined using an empirical relationship with initial litter C:N as reported in (Manzoni et al. 2008) from a meta-analysis of foliar and woody litter decay studies (Eq. 2). This critical C:N is directly linked to microbial CUE (Eq. 3) (Manzoni et al. 2008). For our simulations we assume microbial biomass C:N is 10, consistent with values commonly assumed in decomposition models and empirical syntheses of microbial stoichiometry (Manzoni et al. 2008; Mooshammer et al. 2014).

$$Critical\ C:N = \frac{1}{\left(0.45 \times \left(\frac{1}{Initial\ Dead\ Wood\ C:N}\right)^{0.76}\right)} \tag{2}$$

$$\text{Microbial Carbon Use Efficiency} = \frac{\text{Microbial biomass C:N}}{\text{Critical C:N}} \tag{3}$$

In this study, we refer to microbial CUE as a parameter that governs both C partitioning and N immobilization during decomposition. While CUE is classically defined as a microbial physiological trait, our implementation reflects an effective decomposition-level CUE—similar to the CUE of decomposition described by Zhang et al. (2018). Although we do not explicitly simulate microbial turnover or active biomass, the model tracks C lost through microbial respiration and estimates the fraction of wood C that would enter microbial biomass.

Lastly, we optionally allow for the mortality rate and snag fall rate to vary stochastically across years. To facilitate sensitivity analyses and parameter optimization the model was designed to allow for Monte Carlo type simulations. Model structure as well as parameter values can be varied randomly between model runs within user-defined ranges. We also allow for user-defined disturbance events that specify both the amount of mortality and proportion of CWM from mortality events that remain on site. Disturbance parameters can also vary randomly within a user-defined range between runs.

We do not include physical processes such as fragmentation (e.g., loss of wood by physical breakage), and we do not attempt to simulate the transition of CWM to soil organic matter. These processes occur over a 2–3 decade timeframe in

northern hardwood forests of the White Mountains (Fast et al. 2008), the dominant forest type at Hubbard Brook. Instead, C and N pools continue to be tracked as downed CWM until lost through respiration or mineralization and therefore may overestimate C and N in field-sampled recognizable CWM.

Site description

We simulated C and N dynamics in CWM at the Hubbard Brook Experimental Forest. Hubbard Brook Experimental Forest is a 3,150-ha northern hardwood forest situated within the White Mountain National Forest in New Hampshire, USA and was established in 1955 by the USDA Forest Service. Since 1963 it has been home to the Hubbard Brook Ecosystem Study (https://hubbardbrook.org/), and since 1988, the Hubbard Brook Long Term Ecological Research Program (LTER). We took advantage of long-term records of C and N fluxes and stocks from Watershed 6, a 13.2 ha watershed used as a biogeochemical reference, referred to here as HBEF-W6.

Long-term records of C and N fluxes through streamflow and from atmospheric deposition, as well as stocks in vegetation and soils have been synthesized by numerous authors to provide estimates of the long-term N budget within HBEF-W6 (Bormann et al. 1977; Whittaker et al. 1979; Yanai et al. 2013; Lovett et al. 2018). These analyses have identified several periods of N imbalance at HBEF-W6. In the 1960s-1970s, there was a roughly 14 kg N ha^{-1} yr^{-1} unaccounted for N source (Yanai et al. 2013). This was during a stage when the forest was actively regrowing and net accumulating more N in biomass than was being deposited through atmospheric deposition. More recently, since the early 1990s, there has been a "missing" N sink of roughly 5.5–11.5 kg N ha^{-1} yr^{-1} (Yanai et al. 2013). This apparent annual N sink can be approximated by subtracting N export via streamflow from N inputs via atmospheric deposition, consistent with long-standing N budget analyses at Hubbard Brook. We compare this approximation to model predictions of N fluxes into and out of CWM.

Previous work at Hubbard Experimental Forest has also included a 24-year wood decomposition study of the three dominant species in HBEF-W6 – *Acer saccharum, Betula alleghaniensis*, and *Fagus grandifolia*—see Johnson et al. (2014) for the first 16 years. This study provided estimates of mass loss rates from decaying CWM and initial N and C contents for model parameterization, as well as patterns of N retention and release for model testing. In addition, Arthur et al. (1993) measured N concentration and N retention in downed logs 23 years after a harvest experiment, offering an independent benchmark of long-term N retention dynamics from Hubbard Brook. Measurements of the mass of the standing dead tree pool have occurred periodically since the 1970s, while the mass of the downed CWM pool was measured in 1978, 1995, and 2016. These periodic inventories of CWM stocks over roughly 40 years provided observations for model comparison.

Model parameterization

Default parameter values and the range of parameter values used in sensitivity analyses are listed in Supplemental Table 1. Many of the default parameter estimates were drawn from previous work at Hubbard Brook Experimental Forest (see Supplementary Information (SI) for more detail). For the default parameterization most parameters were held constant over the 500-year simulation period with the exception of wood production. To constrain modeled dead wood inputs and ensure realistic trajectories of CWM accumulation, we estimated aboveground woody net

Table 1 Summary of Model Simulations

Simulation	Purpose	Parameters Varied
1. Cohort-Level Validation	Evaluate model accuracy in simulating N retention and release during decay	Critical C:N, %N, decay rate constant
2. HBEF-W6 Monte Carlo Scenario	1) Validate biomass and dead wood dynamics 2) Assess CWM contribution to N imbalance 3) Quantify parameter sensitivity	± 25% variation in all model parameters; ± 50% mortality, ± 25% removal during 4 disturbances
3. C:N; Microbial CUE	Isolate the effect of microbial CUE on C and N stocks and fluxes	Critical C:N varied 25–325 (microbial CUE of 0.40–0.03)

primary production (NPP) based on long-term wood production and biomass patterns at Hubbard Brook (Whittaker et al. 1974; Fahey et al. 2005; Siccama et al. 2007; Campbell et al. 2013). Specifically, following stand-replacing disturbances or harvests, we simulated an initial low-NPP phase associated with stand reestablishment, a subsequent rise to peak NPP early in stand development, and a decline to a stable, mature-forest NPP rate (see SI, Section S1).

To parameterize wood turnover including mortality, we assumed that the relatively stable live woody biomass observed at HBEF-W6 since the late 1980s (170–190 Mg ha^{-1}; Hubbard Brook data archive) reflects a near steady-state condition. With this assumption, an annual wood turnover rate of 1.7–1.9% is required to balance an assumed mature-forest aboveground woody NPP rate of 320 g C m^{-2} yr^{-1}. We applied a constant annual mortality rate of 1.8% for the default parameterization. Although field-based estimates of dead wood inputs are somewhat lower (Gosz et al. 1972; Siccama et al. 2007; van Doorn et al. 2011), they likely underestimate true turnover due to unmeasured decay losses from standing dead material and attached dead branches on live trees (see SI, Section S1).

Site-specific wood decay parameters were informed by values reported for the HBEF in Johnson et al. (2014) and Arthur et al. (1993). To improve model fit, we used inverse parameter optimization to estimate the decay rate constant by fitting a single exponential decay model to observed trajectories of C and N over time. During this optimization, both the decay constant and the critical C:N thresholds for wood and bark were allowed to vary to best replicate the observed N retention patterns from Johnson et al. (2014). The resulting best-fit parameter set was then validated against independent field data on mass loss from decomposing logs in HBEF-Watershed 2, as reported by Arthur et al. (1993) (see SI, Section S1). Site-specific initial dead wood and bark N concentrations were taken from Johnson et al. (2014). Parameterization of the critical C:N can be user-defined but by default is estimated based on initial wood and bark C:N using the relationship found in Manzoni et al. (2008) (Eq. 2).

We used a default limit value of 0 but investigated the influence of this parameter by allowing the limit value for wood decay to vary between 0–10% based on the assumption that litter with lower N concentrations tend towards low limit values to decay (see SI, Section S1). Parameterization of the bark fraction of wood biomass was estimated from species-specific data (Clausen and Godman 1969; Smith 1969; Whittaker et al. 1974; Evans et al. 2004). In these studies, bark fraction varied minimally above tree diameters of 10 cm for the three dominant species found within HBEF-W6. Estimates of snag fall rates were taken from (Vanderwel et al. 2006; Hilger et al. 2012; Russell and Weiskittel 2012; Battles (unpublished)). The timing and amount of biomass lost during harvest, hurricane, and ice storm disturbances followed those outlined by Bernal et al. (2012).

Model simulations

We used a series of model simulations to evaluate whether CWM contributes to the long-standing N imbalance observed in HBEF-W6. We also sought to determine the range of microbial CUE (represented as critical C:N) values most consistent with observed N dynamics in CWM, and to assess how CUE influences the capacity of dead wood to immobilize N and the fate of wood-derived C. Each simulation ran for 500 years, beginning with a 300-year spin-up period (1600–1900) during which time live and dead wood pools approached steady-state conditions, followed by a 200-year period (1900–2100) that included multiple disturbance events.

First, to evaluate whether the model realistically simulates N retention and release during wood decay, we ran a simulation using default HBEF-W6 parameters and examined outputs at the individual cohort level. Most parameters were held constant, while decay rate constants, initial wood and bark %N, and critical C:N thresholds were allowed to vary. We compared modeled N dynamics to observations from two empirical studies: (1) a 24-year decomposition experiment tracking net N retention and loss in logs of the three dominant tree species at HBEF-W6 (Johnson et al. 2014), and (2) measurements of %N and N retention in downed logs 23 years after harvest (Arthur et al. 1993). Empirical critical C:N values were by default calculated using Eq. 2 and initial substrate chemistry, but also calculated using an inverse parameter optimization to identify best-fit thresholds for wood and bark (see SI, Section S1). Comparisons between empirically derived and best-fit

critical C:N provided a basis for evaluating whether empirically derived critical C:N were sufficient to reproduce observed microbial N dynamics and supported their application in subsequent simulations.

Second, we conducted a simulation consisting of 5,000 Monte Carlo iterations to evaluate the potential contribution of CWM to the N imbalance observed at HBEF-W6 since the 1990s. This simulation incorporated four major disturbance events adapted from Bernal et al. (2012): historical harvests in 1906 and 1917, the 1938 hurricane, and the 1998 ice storm. For each event, tree mortality was allowed to vary by ± 50% from default estimates, and the fraction of harvested biomass removed by ± 25% (see SI, Section S1). All other model input parameters were randomly varied ± 25% around HBEF-W6 default values, and the model structure included a standing dead phase and explicit separation of bark and wood. This simulation addressed three objectives: (1) to test model parameterization and structure through comparison with long-term observations of aboveground productivity, biomass, and standing and downed dead wood within HBEF-W6; (2) to evaluate the contribution of CWM to the watershed-scale N imbalance by comparing modeled N fluxes to observed atmospheric inputs and stream N outputs; and (3) to quantify the relative influence of each input parameter on modeled N fluxes and CWM dynamics through permutation-based sensitivity analysis using Random Forest regression. Details on the Random Forest model fitting, data structure, and the sensitivity analysis are provided in SI, Section S2.

In a third simulation experiment, we isolated the influence of microbial CUE by holding all parameters constant at HBEF-W6 default values except for the critical C:N of wood and bark. While many ecosystem models assume decomposer CUE values > 0.20 (Zhang et al. 2018), empirical studies suggest that CUE is lower for wood-decomposing fungi due to the high C:N of woody substrates. To reflect this difference, we varied critical C:N from 25 (representative of N-rich litter) to 325 (representative of N-poor, woody tissues). These values correspond to microbial CUEs ranging from 0.40 to 0.031. We evaluated how variation in critical C:N (and associated CUE) affected N stocks in standing and downed dead wood, N fluxes in relation to the long-term watershed imbalance, and the partitioning of C between microbial growth and respiration.

Results

The results are organized into three sections: 1) comparison of model output with empirical observations to assess model performance; 2) evaluation of the potential for CWM to account for the watershed-scale N imbalance at HBEF-W6 and identification of key parameters influencing model outcomes; and 3) exploration of how variation in microbial CUE affects simulated dead wood C and N stocks and fluxes.

Model comparison with observations

We assessed model performance by comparing simulated outputs to empirical observations at both the cohort and ecosystem scale. Cohort-level simulations were used to evaluate N retention and release during wood decay, while full-site simulations were used to assess long-term patterns in aboveground biomass, productivity, and dead wood pools under historical disturbance regimes.

For clarity, we briefly restate key model assumptions relevant to N immobilization and mineralization before presenting the results. Our model, similar to others that track nutrient dynamics during decomposition, uses a critical C:N threshold to determine the transition between net N immobilization and mineralization. When substrate C:N exceeds the critical threshold, the model simulates net N immobilization; below this threshold, net mineralization occurs. We evaluated the model's ability to simulate net N dynamics in decaying wood by comparing output from individual model cohorts to observed trajectories of net N retention and release from a 24-year wood decay experiment of the three dominant tree species at HBEF-W6 (Johnson et al. 2014). These comparisons allowed us to assess whether empirically derived critical C:N values, calculated using initial wood and bark chemistry and Eq. 2, were sufficient to reproduce observed N dynamics. In addition, we applied inverse parameter optimization to evaluate how closely the empirically derived critical C:N values aligned with best-fit thresholds under our model structure.

For bark, the empirically derived critical C:N was 58, based on an initial bark C:N of 72. This led the model to simulate a brief phase of early N immobilization (a 3% increase from initial N content) (Fig. 2). While Johnson et al. (2014) observed no net N accumulation in bark, the differences between simulations and observations were minor given the sensitivity of the model to stoichiometric thresholds and the precision of the immobilization measurements. Inverse parameter optimization yielded a higher best-fit critical C:N of 126—consistent with observations of immediate net mineralization.

The empirical and optimized critical C:N values for wood were more closely aligned (234 and 271, respectively) than for bark, and the model reproduced wood-N retention with high accuracy using the empirical parameterization ($R^2 = 0.88$). The empirical parameterization predicted a peak retention of 22% above the initial N content after 6 years—reasonably close to the 16% peak observed after 3 years and the 15% peak obtained with the optimized C:N (Fig. 2). We explored a wide but realistic parameter space by constraining critical C:N to values > 150 (microbial CUE < 0.07)—appropriate for woody substrates. Even within this restricted range, peak immobilization could still exceed observations by ~ 50% in some runs (e.g., critical C:N = 150, CUE = 0.067), underscoring the model's sensitivity to this threshold (Fig. 2). Simulations using low critical C:N = 50 (CUE = 0.20) produced peak immobilization more than 400% above the original N content (not shown). The empirical critical C:N for wood (234), derived using Eq. 2, corresponds to a microbial CUE of 0.043 and produced dynamics that closely matched observations (Fig. 2).

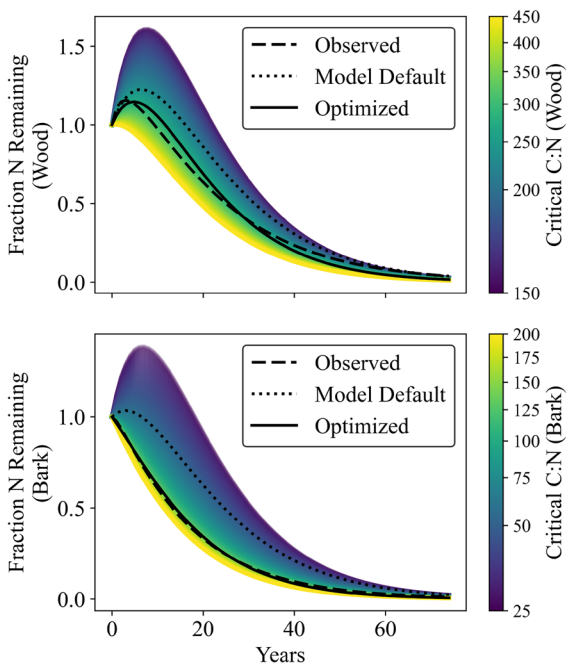

Fig. 2 Modeled N retention trajectories for wood (top) and bark (bottom) from a representative simulated cohort, showing variation across a range of critical C:N. Simulations used a fixed decay rate ($k = 0.09\ yr^{-1}$), with color gradients indicating the critical C:N value applied. Dashed lines show observed values; dotted and solid black lines represent simulations using empirically derived (model default) and optimized parameters, respectively

We also evaluated model performance against independent observations from Arthur et al. (1993), who measured N retention and wood %N in downed logs 23 years after clearcutting at HBEF Watershed 2. Because their data did not distinguish wood and bark, we simulated combined dead wood and bark chemistry using appropriate weighted parameters and model structure. The observed fraction of initial N remaining after 23 years was 0.69, while the median modeled value was 0.67. Observed wood N% was 0.70% ± 0.20%, compared to a simulated value of 0.71% (Fig. 3).

Together, these comparisons of model predictions with measurements from Johnson et al (2014) and Arthur et al. (1993) suggest that the empirical approach to estimating critical C:N provides a reasonable approximation of microbial N dynamics within HBEF-W6 and is appropriate for simulations that span a range of substrate chemistries. To assess the potential for woody material to reconcile the N imbalance at HBEF-W6, we therefore adopted the empirically derived critical C:N calculation for all 5,000 Monte Carlo simulations, which allowed wood and bark chemistry to vary by run.

We next assessed model performance for live biomass and productivity, comparing simulated trajectories against long-term measurements at HBEF-W6. Aboveground woody biomass and wood production were parameterized to follow long-term trends observed at the Hubbard Brook Experimental Forest. The model reproduced the rise and stabilization of live woody biomass following disturbance, with a mean bias of + 1.7 Mg ha^{-1} and a mean absolute error of 6.4 Mg ha^{-1} relative to repeated measurements from HBEF-W6 (1965–2022).

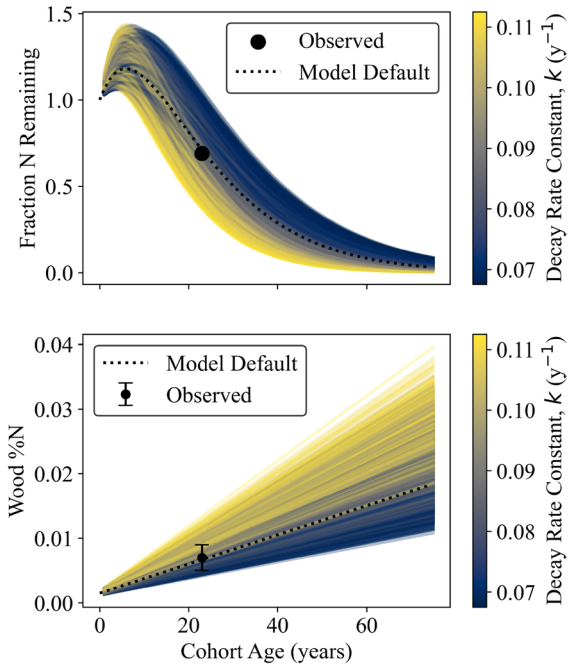

Fig. 3 Modeled N dynamics in downed CWM cohorts compared to observations from Arthur et al. (1993). Each line represents a simulation from a representative cohort, with color indicating the decay rate constant (k). Simulations allowed the decay rate, initial wood %N and critical C:N to vary randomly by ± 25% around default values for HBEF-W6. (Top) Fraction of initial N remaining over time. (Bottom) Wood N concentration (%N). Observed values at year 23 are shown as black circles (with error bars for %N). The dashed black line shows the default model simulation using empirically derived parameters

These results confirm that the model accurately tracked live biomass (SI Fig. S1), and that simulated wood production followed expected successional patterns, with productivity rising post-disturbance and declining to a mature forest rate of 3.20 Mg ha^{-1} yr^{-1}, consistent with recent inventory-based estimates (SI Fig. S2). The model also reproduced historical reconstructions of productivity based on tree ring data from (Whittaker et al. 1974), with a modest positive bias (0.23 Mg ha^{-1} yr^{-1}) consistent with known underestimates in tree-ring data due to survivor bias (Brienen et al. 2012). While these comparisons reflect parameterized behavior rather than independent validation, they provide confidence that modeled turnover and dead wood inputs are grounded in observed productivity and biomass trajectories.

Finally, we evaluated model estimates of standing dead and downed CWM against field observations of coarse woody pools through time. Standing dead and downed CWM were emergent properties of the model and compared well with independent field data. Given the limited temporal resolution of observations and the stochastic nature of tree mortality events, we focused on comparing mean values and ranges across a 40-year period when observations were available (Fig. 4). For standing dead trees, the mean of observed values from 1977–2017 was 15.6 Mg ha^{-1} (range: 8.6–25.4), while the median model simulation was 15.0 Mg ha^{-1} over the same period, with an interquartile range (25th-75th percentile) across 5000 simulations of 13.2–17.4 Mg ha^{-1}. Downed CWM estimates from field surveys ranged from 16–32 Mg ha^{-1}, accounting for buried and partially decomposed material (see SI, Section S1). Simulated downed CWM (1975–2020) averaged 25.6 Mg ha^{-1}, with an interquartile range of 21.8–30.4 Mg ha^{-1}—within the observational envelope (Fig. 4). These results support the model's ability to represent mortality, decay, and long-term dead wood dynamics.

The potential of dead wood to resolve the N imbalance within HBEF-W6

Using our full wood decay model, we assessed the potential for CWM to account for the long-standing N imbalance observed at HBEF-W6 (Fig. 5). Modeled net N increases in the dead wood pool averaged 0.68 kg N ha^{-1} yr^{-1} between 1992 and 2007 (excluding 1998, a known disturbance year), representing less than 10% of the ~ 8.4 kg N ha^{-1} yr^{-1} "missing" N sink reported by Yanai et al. (2013). Over the broader 1975–2025 window, mean modeled fluxes were lower still, averaging 0.51 kg N ha^{-1} yr^{-1}, indicating that while CWM may contribute to ecosystem N retention, it by itself likely does not account for a large proportion of the observed imbalance.

The model's estimates of the N flux to dead wood during 1992–2007 (mean of 0.68 kg N ha^{-1} yr^{-1}) are between those assumed by (Yanai et al. 2013) for recognizable downed coarse dead wood (0.10 kg N ha^{-1} yr^{-1}) and increases in forest floor N (1.7 kg N ha^{-1} yr^{-1}) over the 1992–2007 period. Modeled estimates of net N flux to dead wood decline over time and converge to near zero by the end of the simulation period.

The contribution of grouped model parameters to explained variance varied over time and by output metric (Fig. 6). For net N flux to and from CWM, parameter importance shifted dynamically, from early-century

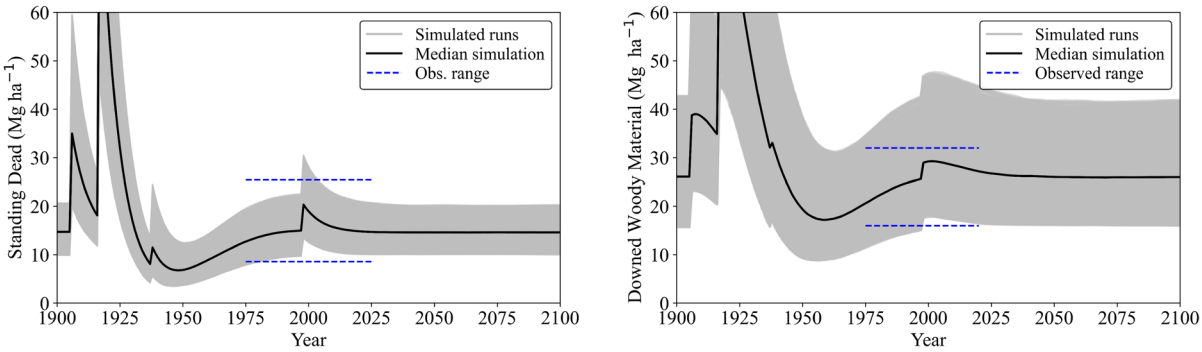

Fig. 4 Comparison of simulated and observed stocks of standing dead wood (left) and downed CWM (right) in HBEF-W6. The shaded gray region shows the range of outputs from 5,000 Monte Carlo type runs in which input parameters were varied randomly by ± 25% around default values. The solid black line represents the median of simulated runs, and the dashed blue lines indicate the observed range of field measurements

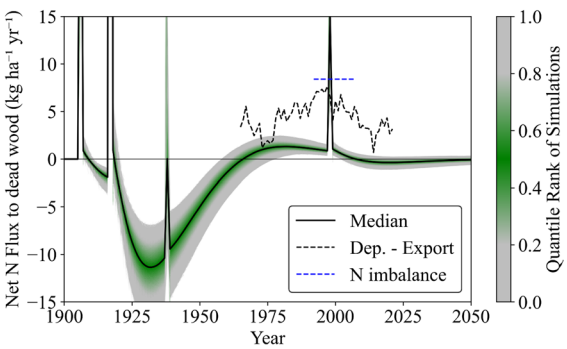

Fig. 5 Simulated net N flux to (positive values) or from (negative values) CWM at HBEF-W6 from 1900 to 2050, based on 5,000 Monte Carlo simulations in which input parameters were varied randomly by ± 25%. The dashed black line is a proxy for the N imbalance observed at HBEF-W6 (N deposition—stream N export) and the dashed blue line is the N imbalance estimated by Yanai et al. (2013) for 1992–2007. Gray to green points represent the output from individual model runs with colors representing a quantile ranking of each run and the solid black line the median of all runs

dominance by disturbance-related mortality towards an increasing influence of wood %N and wood production after 2000. For C transferred to microbial biomass, microbial CUE emerged as the most influential parameter, highlighting the role of microbial stoichiometric thresholds on the fate of wood-derived C. Dead wood N stocks were most strongly influenced by decay rate, though microbial CUE, wood %N, and wood production also contributed substantially. Dead wood C stocks were consistently shaped by decay rate, wood production, and disturbance-related mortality throughout the simulation. Together, these results indicate that different components of dead wood C and N cycling respond to distinct parameters, with stoichiometric traits—particularly microbial CUE and wood chemistry—playing an increasingly important role in regulating C and N fluxes under near steady-state conditions.

Influence of microbial carbon-use efficiency

Because many current forest ecosystem models parameterize wood decay similar to the decay of other organic matter types, with microbial CUE higher than 0.20 (Zhang et al. 2018), for this set of simulations we allowed the critical C:N of wood and bark (microbial CUE) to vary from values more typical of N-rich litter to those suggested for wood and bark components (Eq. 2; Manzoni et al. 2008). Near-steady state N stocks in dead wood varied from ~ 125 kg N ha^{-1} at a critical C:N more typical of wood decomposers (or microbial CUE ~ 0.04), to > 800 kg N ha^{-1} at a critical C:N more typical of N-rich litter (or microbial CUE of ~ 0.40) (Fig. 7). Varying the critical C:N also had a dramatic effect on net N fluxes to the CWM pool during the post-harvest simulation period (Fig. 7). Parameterizing the model with low microbial CUE more typical of wood decomposers resulted in relatively small annual net N fluxes to CWM during this period (< 1 kg N ha^{-1} yr^{-1}). Model simulations with higher microbial CUE resulted in large net fluxes to CWM (> 5 kg N ha^{-1} yr^{-1}), at times exceeding the N imbalance observed in HBEF-W6 (Fig. 7).

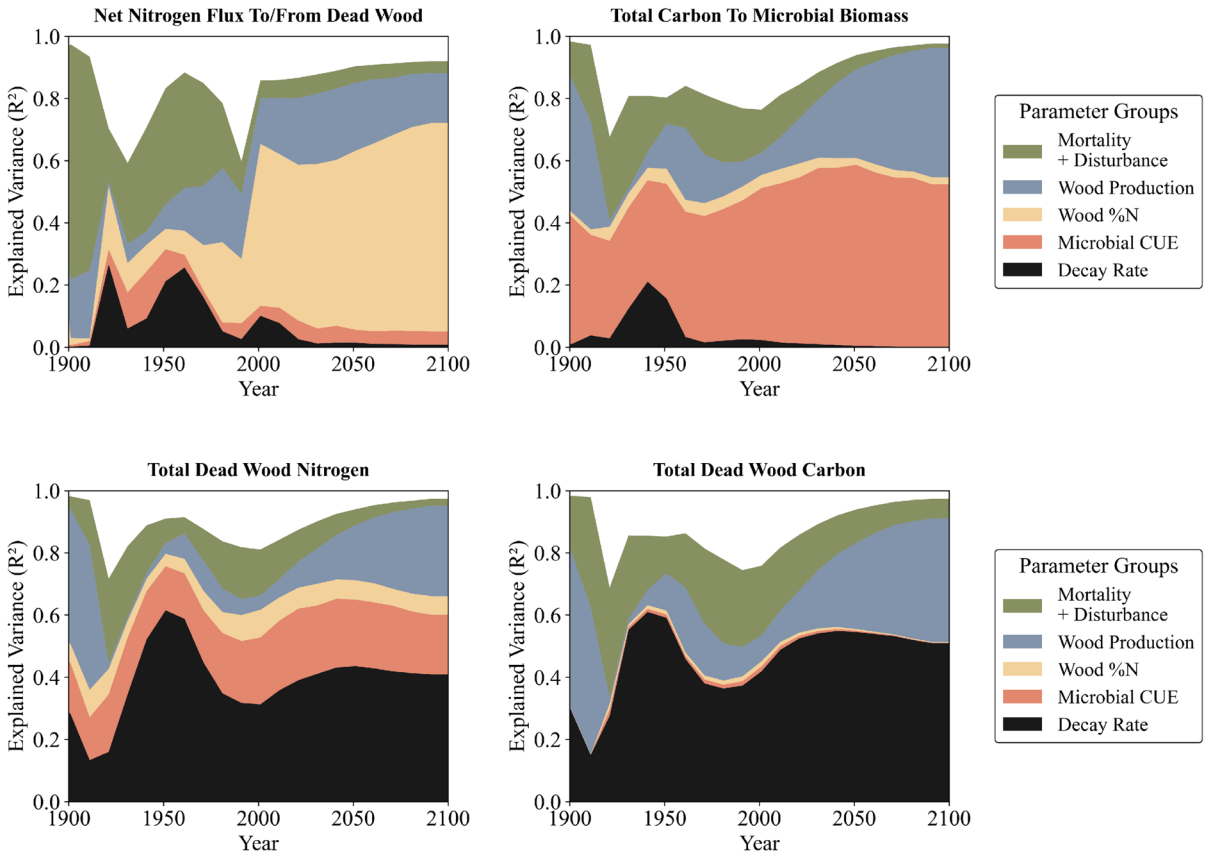

Fig. 6 Absolute importance of grouped model input parameters in explaining variance (R^2) in four key outputs over time, based on Random Forest regression with permutation importance. Panels show the proportion of variance explained by parameter groups for (top left) net nitrogen flux to/from dead wood, (top right) total C transferred to microbial biomass, (bottom left) total N in CWM, and (bottom right) total C in CWM. Importance scores were derived from 5,000 Monte Carlo-type simulations at HBEF-W6, aggregated to decadal means. Values represent absolute importance (relative contribution scaled by model R^2), illustrating which processes most strongly influenced model behavior across successional stages and disturbance regimes

Changes in the critical C:N also had a large impact on the amount of C entering the microbial pool, a likely source of stabile soil organic matter in these ecosystems (Prescott and Vesterdal 2021). At near-steady-state conditions, C entering the microbial pool after 300 years ranged from <0.06 Mg C ha^{-1} yr^{-1} at low microbial CUE (0.04) to >0.60 Mg C ha^{-1} yr^{-1} with a CUE of 0.40. This led to large differences in the cumulative amount of C respired from decaying wood versus the cumulative amount of C entering the microbial pool over time (Fig. 8).

Discussion

Can dead wood explain the N imbalance at HBEF-W6?

A central goal of this study was to evaluate whether CWM could account for the long-standing N imbalance observed at HBEF-W6. Consistent with our first hypothesis, our model simulations suggest that CWM is unlikely to explain the majority of this imbalance. This is largely due to the relatively rapid decay rate of CWM at HBEF-W6 and the empirically derived critical C:N (and low microbial CUE), which limit N immobilization within individual cohorts to less than

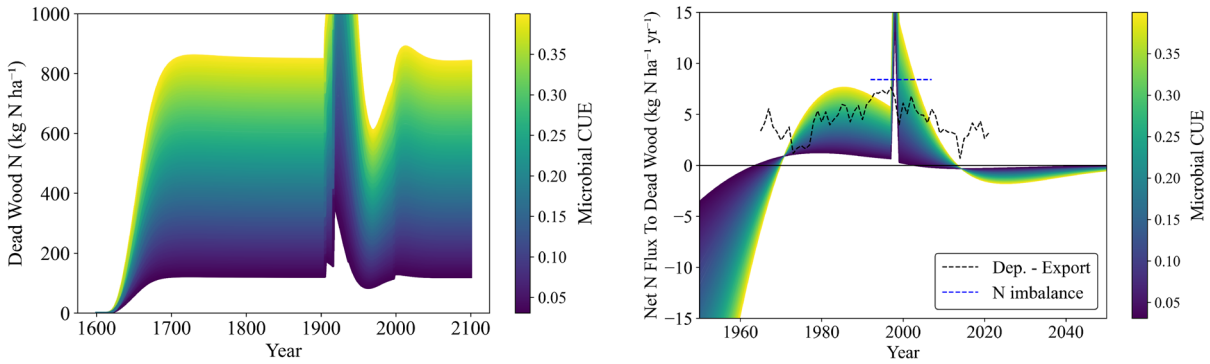

Fig. 7 Results of model simulations that varied only microbial CUE (critical C:N) from values more typical for wood decay (<0.10) to those more typical for N-rich litter (up to 0.40). Left: N stocks in CWM over the entire simulation period. Right: N flux to/from CWM from 1950–2050, with the dashed black line is a proxy for the N imbalance observed at HBEF-W6 (N deposition minus stream N export), and the dashed blue line is the N imbalance estimated by Yanai et al. (2013) for 1992–2007

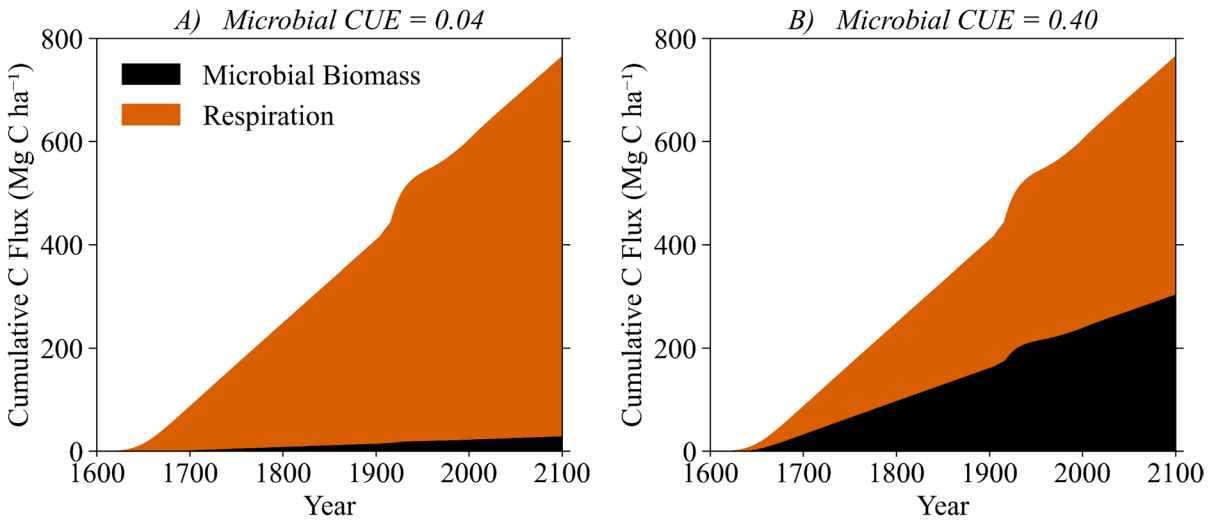

Fig. 8 Simulated partitioning of cumulative wood-derived C between microbial biomass and respiratory loss under default HBEF-W6 parameterization while varying microbial CUE between 0.04 (left) and 0.40 (right). Colored wedges represent modeled cumulative C fluxes: black = C entering microbial biomass; orange = C lost via respiration

a decade—consistent with observations from Johnson et al. (2014).

At the ecosystem scale, the net N flux to and from CWM reflects the balance between 1) net N additions associated with increases in the size of the CWM pool due to mortality and turnover 2) N immobilization by newly added woody material, and 3) N mineralization from older, decaying material. Although individual cohorts of dead wood tend to immobilize N for several years following input (<10 years), the ecosystem-scale signal is shaped by the composite effect of all existing cohorts, many of which are already undergoing net N mineralization.

For example, the disturbance pulses associated with the 1917 harvest introduced large quantities of CWM that immobilized N initially. However, the ecosystem-level N flux rapidly shifted back to net mineralization, not because those new inputs failed to immobilize N, but because they were outweighed by ongoing mineralization from older CWM already

well into decay. This dynamic is clearly illustrated in Fig. 9, where the sharp peaks in N input are quickly followed by a return to negative net flux. These results indicate that even large disturbances do not produce a sustained N sink when the background pool is already dominated by decomposing wood.

In contrast, during the mid- to late twentieth century, forest recovery and increasing live biomass led to a steady rise in inputs from background mortality and turnover. This gradual buildup of the CWM pool led to a period where N inputs to CWM temporarily exceeded mineralization losses, resulting in ecosystem-level net N accumulation (e.g., 1970s–2000s). Yet this simulated period of net N accumulation in CWM was transient. Once the CWM pool reached dynamic equilibrium in the early 2000s, the net N flux again stabilized near zero, with inputs and mineralization roughly in balance (Fig. 9). These results suggest that while CWM can temporarily act as a N sink under specific forest developmental conditions, they support our initial hypothesis that its contribution to the long-term N imbalance at HBEF-W6 is limited. The combination of rapid turnover and dominant mineralization from aging wood cohorts constrains its role as a persistent ecosystem-scale N sink.

While CWM is unlikely to account for the long-term N imbalance at HBEF-W6, previous syntheses have suggested that long-term N retention in soil organic matter may represent a more plausible missing sink at this site (Lovett et al. 2018).

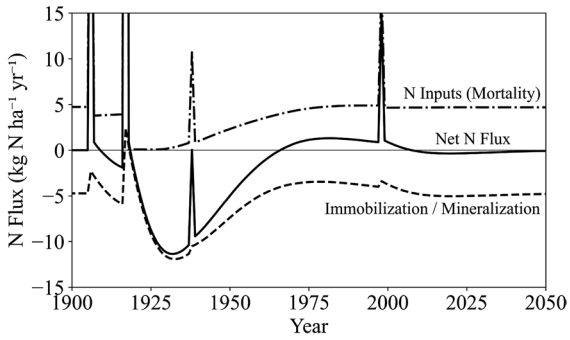

Fig. 9 Simulated N fluxes associated with CWM at HBEF-W6 from 1900 to 2050. The solid line represents the net ecosystem-scale N flux to/from the CWM pool, the dashed line indicates net N immobilization (positive values) or mineralization (negative values), and the dot-dashed line shows N inputs from tree mortality and turnover

Future work that integrates microbial processing, mineral-organic interactions, and long-term soil N stabilization may be critical for resolving remaining uncertainties in ecosystem-scale N budgets.

Modeling approach and microbial CUE

Although our primary objective was to evaluate whether CWM could help reconcile the N imbalance observed in HBEF-W6, model development also highlighted the importance of appropriately parameterizing microbial CUE and stoichiometric thresholds. We used an empirical approach based on initial substrate chemistry to estimate CUE via critical C:N, allowing it to vary with initial wood and bark stoichiometry. When applied to CWM, this empirical relationship tended to predict a longer period of N immobilization than was observed empirically, consistent with a recent synthesis indicating that N release from wood often occurs earlier than expected based on relationships derived using primarily foliar litter (Wijas et al. 2025). While CUE is often defined as a microbial physiological trait, our implementation reflects an effective decomposition-level CUE -governing both C partitioning and N immobilization—consistent with the concept of CUE of decomposition described by Zhang et al. (2018). This flexible, stoichiometry-based representation enabled the model to reproduce observed N retention and release patterns in decaying wood, despite its relative simplicity.

In contrast, many existing litter decay models assume microbial CUE is fixed above 0.20 and do not allow CUE to vary with substrate stoichiometry (Zhang et al. 2018). When we parameterized our model with a fixed CUE of 0.20 or higher (equivalent to a critical C:N of 50 or lower), it predicted substantially more N immobilization in CWM—enough to fully account for the N imbalance at HBEF-W6. However, under these high-CUE assumptions, the model simulated N retention and release dynamics that were inconsistent with empirical observations, including results from a long-term wood decay experiment (Johnson et al. 2014) and N contents measured in situ 23 years after clearcutting (Arthur et al. 1993). These findings support previous work showing that microbial CUE varies with litter stoichiometry and is often below 0.10 for microbes decomposing high C:N woody

substrates (Manzoni et al. 2008, 2012). Our results indicate that incorporating a flexible, substrate-sensitive CUE improves model realism and avoids overestimating the role of CWM as a persistent N sink, consistent with our second hypothesis that low microbial CUE (< 0.10) best reproduces observed N and C dynamics during wood decay.

Beyond its implications on N dynamics, in our simulations microbial CUE was the dominant control on the modeled partitioning of wood-derived C between microbial biomass and respiratory loss, even when microbial CUE was constrained to values more appropriate for wood decomposers (Fig. 8). Under low microbial CUE values (< 0.10), the model predicted that only a small fraction of wood-derived C would be routed to microbial biomass, with the majority lost via respiration. If microbial processing represents a primary pathway for the formation of stable soil organic matter, as widely hypothesized (Prescott and Vesterdal 2021), these results imply that CWM may contribute less to long-term soil C storage through microbial assimilation than N-rich litter.

This interpretation is consistent with results from isotopically labeled litter decomposition experiments in a central New York forest (Fahey et al. 2021, 2024), which found that, in contrast to foliar and root litter, little woody litter C was recovered in soil organic matter pools after a decade of decomposition and nearly complete decay of the woody litter. Although C losses were not directly measured in those studies, the limited recovery of woody C in soil pools suggests substantial respiratory loss, consistent with the low effective microbial CUE values (high critical C:N) used in our modelling. Taken together, these observations support our second hypothesis that low microbial CUE (< 0.10) best reproduces observed N and C dynamics during wood decay.

Although this study focused on a northern hardwood forest, the mechanism linking high substrate C:N to low microbial CUE is not unique to HBEF-W6. Additional simulations parameterized for a conifer-dominated forest system (see Supplementary Information, Section S3) showed longer N immobilization at the cohort scale but similarly limited ecosystem-scale N sinks due to the transition to net mineralization over decadal timescales.

While our empirical approach captured key features of C and N dynamics during wood decay, there are additional microbial mechanisms that warrant further investigation, particularly for applications beyond the HBEF-W6 context. One such area is the potential role of mineral N availability in shaping microbial CUE and decay rates. In this study, CUE (and the associated critical C:N) was parameterized as a function of initial litter chemistry, and decay rates were constrained by observations. However, evidence suggests that mineral N availability can influence microbial CUE (Manzoni et al. 2017; Zhang et al. 2018), and that N limitation can suppress both N immobilization and decay rates (Averill and Waring 2018). Incorporating dynamic links between mineral N and microbial physiology could improve future predictions, especially in ecosystems undergoing N oligotrophication (Groffman et al. 2018) or recovering from high historical N deposition.

An additional limitation of our modeling approach is that, although microbial CUE was allowed to vary with initial litter chemistry, wood was parameterized using site-level, species-aggregated chemistry. In reality, tree species can differ in initial N content and N immobilization dynamics during decay (Johnson et al. 2014). Although our model allowed for a flexible microbial CUE based on initial litter chemistry, microbial CUE was held constant throughout the decay of each wood cohort. In reality, microbial CUE may evolve as microbial communities shift and substrate stoichiometry changes. Factors such as priority effects, microbial competition, and interactions with soil resources are known to shape decomposer community dynamics (van der Wal et al. 2013, 2016; Hiscox et al. 2015, 2018). As wood loses C and narrows in C:N, stoichiometric demands ease, potentially allowing for increased CUE. However, CUE of decomposition is influenced by more than stoichiometry: microbial competition can reduce CUE through the production of C-rich defense compounds (Maynard et al. 2017), and recent work suggests microbes may also rely on other strategies, such as flexible biomass C:N, nutrient recycling, or enzyme specialization (Mooshammer et al. 2014; Manzoni et al. 2021). More data on microbial traits during wood decay are needed to assess the importance of these potential adaptations. Nonetheless, our current representation of CUE, based on initial substrate chemistry, proved sufficient to capture key observed patterns in N dynamics at HBEF-W6.

Sensitivity of dead wood C and N dynamics to model parameters and structure

Our ability to parameterize and evaluate the model at HBEF-W6 benefited from extensive long-term data on wood chemistry, decay rates, biomass pools, and N fluxes. This empirical foundation enabled both model testing and meaningful comparison to observations. Our sensitivity analysis of grouped input parameters revealed that different mechanisms likely drive C and N dynamics in CWM at different stages of forest development (Fig. 6).

Disturbance-driven mortality and biomass recovery exerted dominant influence on all outputs early in succession, particularly during periods of major biomass loss (e.g., harvests in the early twentieth century). However, as the forest matured and stand structure stabilized, microbial and chemical constraints (wood %N and microbial CUE, which in our model is estimated from %N) emerged as primary controls for N flux to/from CWM and the fate of CWM carbon. Microbial CUE can also have a large influence on CWM N stocks (Figs. 6 and 7). In contrast, CWM decay rates and inputs from live wood turnover dominated uncertainty in total CWM C stocks. Model structural assumptions can also play an important role in shaping long-term dynamics. Simulations that included a recalcitrant decay pool or explicitly represented standing dead wood produced longer residence times and higher cumulative C and N stocks in CWM pools, with relatively modest effects on annual N fluxes (see SI, Sect. 3).

These shifting sensitivities highlight that the dominant drivers of model outputs are not static but evolve with forest developmental stage and process of interest. For model application beyond HBEF-W6, these results provide guidance on which parameters are most critical to constrain under different ecological contexts and suggest that parameter prioritization should be output-specific and time-dependent.

Conclusions

Nitrogen is a critical nutrient for forest productivity and timber production. Processes that immobilize or release N, such as microbial activity during wood decay, can influence long-term soil fertility, nutrient retention, and sustainable yield. In this study, we evaluated whether CWM could account for the long-standing N imbalance observed at HBEF-W6, where N inputs consistently exceed known outputs.

Our results demonstrate that while CWM can temporarily act as a N sink under specific forest conditions, it is unlikely to account for the long-standing N imbalance observed at HBEF-W6. The rapid decay and limited N immobilization capacity of CWM, particularly under low microbial CUE, suggest that other ecosystem compartments (e.g., soils) or processes likely contribute to the majority of the missing N sink (Lovett et al. 2018).

Within our model framework, a low microbial CUE of decomposition was most consistent with empirical observations and imposed a strong constraint on N retention. This stoichiometry-based representation of microbial CUE also led to the majority of wood-derived C being lost as CO_2, reinforcing the idea that microbial traits substantially influence both C and N cycling in decomposing wood.

These findings emphasize the importance of integrating microbial physiology, substrate chemistry, and ecosystem disturbance history into future efforts to resolve watershed-scale nutrient imbalances. Accounting for these interacting factors is essential for improving biogeochemical models and understanding the long-term fate of nutrients in forested ecosystems.

Acknowledgements We gratefully acknowledge the late Dr. Gary E. Lovett (Cary Institute of Ecosystem Studies; Hubbard Brook Ecosystem Study) for his contributions to the conception of this manuscript and his thoughtful revisions. Gary was an inspiring colleague whose insight into forest ecosystems, generosity, and kindness as a collaborator enriched this work. His dedication to the ecological research community will be greatly missed. This work was conducted at the Hubbard Brook Experimental Forest, which is operated and maintained by the USDA Forest Service, Northern Research Station. The Hubbard Brook Experimental Forest is part of the Hubbard Brook Ecosystem Study. The Hubbard Brook Ecosystem Study is a collaborative effort facilitated by the National Science Foundation's Long Term Ecological Research (LTER) program. The findings and conclusions are those of the authors and should not be construed to represent any official USDA or U.S. Government determination or policy.

Author Contributions AO, SO, MD, CF, CG, AL, designed the study. AO and SO developed the modeling approach.

AO and JH coded the model into python. AO ran model simulations, produced results, and drafted the manuscript. All authors provided oral and written feedback and revised the manuscript.

Funding This work was supported by: National Science Foundation LTER 1114804. National Science Foundation LTER 1637685. National Science Foundation DEB 1257956. National Science Foundation DEB 1257808. National Science Foundation DEB 2224545. Northeastern States Research Cooperative (grant # 23-DG-11242311–020).

Data Availability Model code and default input files are available at: https://github.com/apouimette/Coarse_Wood_Decay_Model_Carbon_Nitrogen

Declarations

Competing Interests The authors have no relevant financial or non-financial interests to disclose.

References

Arthur MA, Tritton LM, Fahey TJ (1993) Dead bole mass and nutrients remaining 23 years after clear-felling of a northern hardwood forest. Can J for Res 23:1298–1305. https://doi.org/10.1139/x93-166

Averill C, Waring B (2018) Nitrogen limitation of decomposition and decay: how can it occur? Glob Change Biol 24:1417–1427. https://doi.org/10.1111/gcb.13980

Berg B, Staaf H (1981) Leaching, accumulation and release of nitrogen in decomposing forest litter. Ecol Bull 33:163–178

Berg B, Ekbohm G, Johansson MB et al (1996) Maximum decomposition limits of forest litter types: a synthesis. Can J Bot 74:659–672. https://doi.org/10.1139/b96-084

Bernal S, Hedin LO, Likens GE et al (2012) Complex response of the forest nitrogen cycle to climate change. Proc Natl Acad Sci U S A 109:3406–3411. https://doi.org/10.1073/pnas.1121448109

Bormann FH, Likens GE, Melillo JM (1977) Nitrogen budget for an aggrading Northern Hardwood Forest Ecosystem. Science 196:981–983

Brais S, Paré D, Lierman C (2006) Tree bole mineralization rates of four species of the Canadian eastern boreal forest: implications for nutrient dynamics following stand-replacing disturbances. Can J for Res 36:2331–2340. https://doi.org/10.1139/X06-136

Brienen RJW, Gloor E, Zuidema PA (2012) Detecting evidence for CO2 fertilization from tree ring studies: the potential role of sampling biases. Global Biogeochem Cycles. https://doi.org/10.1029/2011GB004143

Campbell JL, Bailey AS, Eagar C, et al (2013) Vegetation treatments and hydrologic responses at the Hubbard Brook Experimental Forest, New Hampshire. In: Camp, AE; Irland, LC; Carroll, CJW, eds Long-term silvicultural & ecological studies: Results for science and nanagement Volume 2 Yale University, Global Institute of Sustainable Forestry, Research Paper 013: 1–9 1–9

Chen H, Harmon ME, Griffiths RP (2001) Decomposition and nitrogen release from decomposing woody roots in coniferous forests of the Pacific Northwest: a chronosequence approach. Can J for Res 31:246–260. https://doi.org/10.1139/cjfr-31-2-246

Clausen KE, Godman RM (1969) Bark characteristics indicate age and growth rate of yellow birch. US Forest Service, Research Note NC-75:3

Creed IF, Morrison DL, Nicholas MS (2004) Is coarse woody debris a net sink or source of nitrogen in the red spruce - Fraser fir forest of the southern Appalachians, U.S.A.? Can J for Res 34:716–727. https://doi.org/10.1139/x03-211

Edmonds RL (1987) Decomposition rates and nutrient dynamics in small-diameter woody litter in four forest ecosystems in Washington, U.S. Can J Forest Res 17:499–509

Evans C a., Lucas J a., Twery MJ (2004) Beech Bark Disease: Proceedings of the Beech Bark Disease. In Beech Bark Disease: Proceedings of the Beech Bark Disease 331:60–64

Fahey TJ, Siccama TG, Driscoll CT et al (2005) The biogeochemistry of carbon at Hubbard Brook. Biogeochemistry 75:109–176. https://doi.org/10.1007/s10533-004-6321-y

Fahey T, Bohlen P, Feldpausch TR et al (2021) Tracing carbon flow through a sugar maple forest and its soil components: role of invasive earthworms. Plant Soil 464:517–537. https://doi.org/10.1007/s11104-021-04971-4

Fahey TJ, Heinz AK, Mathisson R et al (2024) How much soil carbon is derived from woody detritus? A ten-year study of ^{13}C incorporation into soil organic matter. Ecosystems 27:867–878. https://doi.org/10.1007/s10021-024-00926-9

Fast AJ, Ducey MJ, Gove JH, Leak WB (2008) Dating tree mortality using log decay in the White Mountains of New Hampshire. North J Appl for 25:154–157

Ganjegunte GK, Condron LM, Clinton PW et al (2004) Decomposition and nutrient release from radiata pine (*Pinus radiata*) coarse woody debris. Forest Ecol Manage 187:197–211. https://doi.org/10.1016/S0378-1127(03)00332-3

Garber SM, Brown JP, Wilson DS et al (2005) Snag longevity under alternative silvicultural regimes in mixed-species

forests of central Maine. Can J Forest Res 35:787–796. https://doi.org/10.1139/x05-021
Gosz JR, Likens GE, Bormann FH (1972) Nutrient content of litter fall on the Hubbard Brook Experimental Forest, New Hampshire. Ecology 53:769–784. https://doi.org/10.2307/1934293
Grier C (1978) A *Tsugaheterophylla – Piceasitchensis* ecosystem of coastal Oregon: decomposition and nutrient balances of fallen logs. Can J Forest Res 8:198–206
Groffman PM, Driscoll CT, Durán J et al (2018) Nitrogen oligotrophication in northern hardwood forests. Biogeochemistry 141:523–539. https://doi.org/10.1007/s10533-018-0445-y
Harmon ME, Franklin JF, Swanson FJ et al (2004) Ecology of coarse woody debris in temperate ecosystems. Adv Ecol Res 34:59–234. https://doi.org/10.1016/S0065-2504(03)34002-4
Harmon ME, Fasth BG, Yatskov M et al (2020) Release of coarse woody detritus-related carbon: a synthesis across forest biomes. Carb Balance Manag 15:1–21. https://doi.org/10.1186/s13021-019-0136-6
Harmon ME (2021) The role of woody detritus in biogeochemical cycles: past, present, and future. | EBSCOhost. https://openurl.ebsco.com/contentitem/10.1007%2Fs10533-020-00751-x?sid=ebsco:plink:crawler&id=ebsco:10.1007%2Fs10533-020-00751-x. Accessed 25 Aug 2025
Hilger AB, Shaw CH, Metsaranta JM, Kurz WA (2012) Estimation of snag carbon transfer rates by ecozone and lead species for forests in Canada. Ecol Appl 22:2078–2090. https://doi.org/10.1890/11-2277.1
Hiscox J, Savoury M, Müller CT et al (2015) Priority effects during fungal community establishment in beech wood. ISME J 9:2246–2260. https://doi.org/10.1038/ismej.2015.38
Hiscox J, O'Leary J, Boddy L (2018) Fungus wars: basidiomycete battles in wood decay. Stud Mycol 89:117–124. https://doi.org/10.1016/j.simyco.2018.02.003
Johnson CE, Siccama TG, Denny EG et al (2014) In situ decomposition of northern hardwood tree boles: decay rates and nutrient dynamics in wood and bark. Can J Forest Res 44:1515–1524. https://doi.org/10.1139/cjfr-2014-0221
Krankina ON, Harmon ME, Griazkin AV (1999) Nutrient stores and dynamics of woody detritus in a boreall forest: modeling potential implications at the stand level. Can J Forest Res 29:20–32. https://doi.org/10.1139/x98-162
Laiho R, Prescott CE (2004) Decay and nutrient dynamics of coarse woody debris in northern coniferous forests: a synthesis. Can J Forest Res 34:763–777. https://doi.org/10.1139/x03-241
Lajtha K (2020) Nutrient retention and loss during ecosystem succession: revisiting a classic model. Ecology 101:1–6. https://doi.org/10.1002/ecy.2896
Law S, Eggleton P, Griffiths H et al (2019) Suspended dead wood decomposes slowly in the tropics, with microbial decay greater than termite decay. Ecosystems 22:1176–1188. https://doi.org/10.1007/s10021-018-0331-4
Lines ER, Coomes DA, Purves DW (2010) Influences of forest structure, climate and species composition on tree mortality across the Eastern US. PLoS ONE. https://doi.org/10.1371/journal.pone.0013212
Lovett GM, Goodale CL, Ollinger SV et al (2018) Nutrient retention during ecosystem succession: a revised conceptual model. Front Ecol Environ 16:532–538. https://doi.org/10.1002/fee.1949
Manzoni S (2017) Flexible carbon-use efficiency across litter types and during decomposition partly compensates nutrient imbalances-results from analytical stoichiometric models. Front Microbiol 8:1–15. https://doi.org/10.3389/fmicb.2017.00661
Manzoni S, Jackson RB, Trofymow JA, Porporato A (2008) The global stoichiometry of litter nitrogen mineralization. Science 321:684–686. https://doi.org/10.1126/science.1159792
Manzoni S, Piñeiro G, Jackson RB et al (2012) Analytical models of soil and litter decomposition: solutions for mass loss and time-dependent decay rates. Soil Biol Biochem 50:66–76. https://doi.org/10.1016/j.soilbio.2012.02.029
Manzoni S, Čapek P, Mooshammer M et al (2017) Optimal metabolic regulation along resource stoichiometry gradients. Ecol Lett 20:1182–1191. https://doi.org/10.1111/ele.12815
Manzoni S, Chakrawal A, Spohn M, Lindahl BD (2021) Modeling microbial adaptations to nutrient limitation during litter decomposition. Front For Glob Change. https://doi.org/10.3389/ffgc.2021.686945
Maynard DS, Crowther TW, Bradford MA (2017) Fungal interactions reduce carbon use efficiency. Ecol Lett 20:1034–1042. https://doi.org/10.1111/ele.12801
Mooshammer M, Wanek W, Zechmeister-Boltenstern S, Richter AA (2014) Stoichiometric imbalances between terrestrial decomposer communities and their resources: mechanisms and implications of microbial adaptations to their resources. Front Microbiol. https://doi.org/10.3389/fmicb.2014.00022
Oberle B, Ogle K, Zanne AE, Woodall CW (2018) When a tree falls: controls on wood decay predict standing dead tree fall and new risks in changing forests. PLoS ONE 13:e0196712. https://doi.org/10.1371/journal.pone.0196712
Palviainen M, Laiho R, Mäkinen H, Finér L (2008) Do decomposing Scots pine, Norway spruce, and silver birch stems retain nitrogen? Can J Forest Res 38:3047–3055. https://doi.org/10.1139/X08-147
Prescott CE, Vesterdal L (2021) Decomposition and transformations along the continuum from litter to soil organic matter in forest soils. Forest Ecol Manag 498:119522
Prescott CE, Corrao K, Reid AM et al (2017) Changes in mass, carbon, nitrogen, and phosphorus in logs decomposing for 30 years in three rocky mountain coniferous forests. Can J Forest Res 47:1418–1423. https://doi.org/10.1139/cjfr-2017-0001
Preston CM, Trofymow JA, Nault JR (2012) Decomposition and change in N and organic composition of small-diameter Douglas-fir woody debris over 23 years. Can J Forest Res 42:1153–1167. https://doi.org/10.1139/X2012-076
Romashkin I, Shorohova E, Kapitsa E et al (2018) Carbon and nitrogen dynamics along the log bark decomposition continuum in a mesic old-growth boreal forest.

Eur J Forest Res 137:643–657. https://doi.org/10.1007/s10342-018-1131-2

Romashkin I, Shorohova E, Kapitsa E et al (2021) Substrate quality regulates density loss, cellulose degradation and nitrogen dynamics in downed woody debris in a boreal forest. Forest Ecol Manag 491:119143. https://doi.org/10.1016/j.foreco.2021.119143

Russell MB, Weiskittel AR (2012) Assessing and modeling snag survival and decay dynamics for the primary species in the Acadian forest of Maine, USA. Forest Ecol Manag 284:230–240. https://doi.org/10.1016/j.foreco.2012.08.004

Siccama TG, Fahey TJ, Johnson CE et al (2007) Population and biomass dynamics of trees in a northern hardwood forest at Hubbard Brook. Can J Forest Res 37:737–749. https://doi.org/10.1139/X06-261

Smith CH (1969) Bark thickness related to tree diameter in sugar maple (acer saccharum marsh). USDA Forest Res Note. 107:1–4. https://doi.org/10.5962/bhl.title.69413

Smyth CE, Titus B, Trofymow JA et al (2016) Patterns of carbon, nitrogen and phosphorus dynamics in decomposing wood blocks in Canadian forests. Plant Soil 409:459–477. https://doi.org/10.1007/s11104-016-2972-4

Sollins P, Cline S, Verhoeven T et al (1987) Patterns of log decay in old-growth Douglas-fir forests. Can J Forest Res 17:1585–1595

Strukelj M, Brais S, Mazerolle MJ et al (2018) Decomposition patterns of foliar litter and deadwood in managed and unmanaged stands: a 13-year experiment in boreal mixedwoods. Ecosystems 21:68–84. https://doi.org/10.1007/s10021-017-0135-y

van der Wal A, Geydan TD, Kuyper TW, de Boer W (2013) A thready affair: linking fungal diversity and community dynamics to terrestrial decomposition processes. FEMS Microbiol Rev 37:477–494. https://doi.org/10.1111/1574-6976.12001

van der Wal A, Klein Gunnewiek PJA, Cornelissen JHC et al (2016) Patterns of natural fungal community assembly during initial decay of coniferous and broadleaf tree logs. Ecosphere 7:e01393. https://doi.org/10.1002/ecs2.1393

van Doorn NS, Battles JJ, Fahey TJ et al (2011) Links between biomass and tree demography in a northern hardwood forest: a decade of stability and change in Hubbard Brook Valley, New Hampshire. Can J for Res 41:1369–1379. https://doi.org/10.1139/x11-063

Vanderwel MC, Caspersen JP, Woods ME (2006) Snag dynamics in partially harvested and unmanaged northern hardwood forests. Can J for Res 36:2769–2779. https://doi.org/10.1139/X06-173

Whittaker RH, Bormann FH, Likens GE, Siccama TG (1974) The Hubbard Brook Ecosystem Study : forest biomass and production. Ecol Monogr 44:233–254

Whittaker RH, Likens GE, Bormann FH et al (1979) The Hubbard Brook Ecosystem Study : forest nutrient cycling and element behavior. Ecology 60:203–220

Wiebe S, Morris D, Luckai N, Reid D (2012) Coarse woody debris dynamics following biomass harvesting: tracking carbon and nitrogen patterns during early stand development in upland black spruce ecosystems. Int J Forest Eng 23:25–32. https://doi.org/10.1080/14942119.2012.10739957

Wijas BJ, Cornwell WK, Oberle B et al (2025) Faster than expected: release of nitrogen and phosphorus from decomposing woody litter. New Phytol 245:2214–2223. https://doi.org/10.1111/nph.20362

Yanai RD, Vadeboncoeur MA, Hamburg SP et al (2013) From missing source to missing sink: long-term changes in the nitrogen budget of a northern hardwood forest. Environ Sci Technol 47:11440–11448. https://doi.org/10.1021/es4025723

Zechmeister-Boltenstern S, Keiblinger KM, Mooshammer M et al (2015) The application of ecological stoichiometry to plant–microbial–soil organic matter transformations. Ecol Monogr 85:133–155. https://doi.org/10.1890/14-0777.1

Zhang H, Goll DS, Manzoni S et al (2018) Modeling the effects of litter stoichiometry and soil mineral N availability on soil organic matter formation using CENTURY-CUE (v1.0). Geosci Model Dev 11:4779–4796